

## EXPERIMENTAL STUDY ON FORCED CONVECTIVE HEAT TRANSFER OF FLOWING GASEOUS SOLID SUSPENSION AT HIGH TEMPERATURE

S. HASEGAWA

Department of Nuclear Engineering, Kyusyu University, Fukuoka, Japan,

R. ECHIGO

Department of Mechanical Engineering, Tokyo Institute of Technology, Tokyo, Japan

K. KANEMARU

Department of Mechanical Engineering, Nagasaki University, Nagasaki, Japan

K. ICHIMIYA

Department of Mechanical Engineering, Yamanashi University, Yamanashi, Japan

M. SANUI

Department of Energy Conversion, Graduate School of Engineering Science, Kyusyu University, Fukuoka,  
Japan

(Received 27 November 1981; in revised form 29 April 1982)

**Abstract**—The results of an experimental study of the forced convective heat transfer to helium-graphite suspension at high temperatures up to 1173K are presented. Entering gas Reynolds number ranges from  $1.0 \times 10^4$  to  $2.0 \times 10^4$  and the particle loading ratio reaches about 4. The ratio of the Nusselt number of the suspension to that of gas alone increases considerably in a range of high loading ratios as the wall temperature increases. Subsequently, two kinds of turbulence promoters (200 and 400 mm pitch twisted tapes) are inserted in the flowing gaseous solid suspensions to make use of the large inertia forces of particles. The current results show that the local heat fluxes with use of the tapes increase significantly with the rise in the wall temperature owing to the radiative effect of the particulate phase.

### 1. INTRODUCTION

Some cooling methods have been so far discussed in high flux heat transfer systems such as high temperature gas reactors and blankets of controlled thermonuclear reactors. The authors have examined the feasibility of gaseous solid suspensions as a cooling medium. In the moderate temperature range, wherein the effects of thermal radiation are negligible, gaseous solid suspensions have been studied extensively and some monographs have been published by Soo (1967) and Boothroyd (1971). Also, Depew & Kramer (1973) have summarized new developments in this field. It is pointed out that the basic features of suspensions are large heat capacity without pressurizing and a relevance to the radiative heat transfer. Further, it has to be emphasized that addition of solids may sometimes change the structure of turbulence remarkably. In order to evaluate the heat transfer characteristics at high temperatures, a series of analytical studies on combined radiative and convective heat transfer of the multiphase flow has been proposed by Echigo & Hasegawa (1972), Echigo *et al.* (1972) and Modest *et al.* (1980). Subsequently, an experimental facility on the "Heat Transfer Loop-Gaseous Solid Suspension at high temperatures (HTL-GSS)" was installed in Kyusu University and some experimental data have been accumulated. In the current paper, the results of the experimental study on the forced convective heat transfer to flowing helium-graphite suspensions both with and without turbulence promoters are presented at high heat fluxes and high temperatures. These results show that the enhanced heat transfer of the suspension medium is successfully confirmed owing to the radiative effect to which the particulate phase might pertain.

## 2. EXPERIMENTAL METHOD

*Selection of suspension*

From the view point of a coolant in a heat transfer system which is subject to high heat flux, the selection of the gaseous phase and particulate material was made. Some dispersed materials such as iron, tungsten and graphite were circulated in this loop together with carrier gases such as air, nitrogen and helium. As a result of the preliminary runs, it was found that iron powder agglomerated and welded to the heating surface at a temperature below the melting point and tungsten particles caused the pipes of the loop to be eroded, especially around the bend. On the other hand, the suspension which is composed of graphite particles and helium gas has had no detrimental effect in the circulation. Therefore, this combination was chosen as a suspension medium throughout the heat transfer experiment and its feasibility as the cooling medium was investigated at high temperatures.

*Particle size distribution*

The particle size distribution of graphite used in the current study is shown in figure 1. The particle diameters ranging from  $4\ \mu\text{m}$  to  $44\ \mu\text{m}$  were measured by Coulter counter, after cutting off particles below the lower edge and sifting particles above  $44\ \mu\text{m}$  of diameter under water. This figure shows the average particle diameter is  $18\ \mu\text{m}$ , which means the 50% cumulative weighted diameter.

*Experimental apparatus*

A schematic diagram of HTL-GSS (Heat Transfer Loop-Gaseous Solid Suspension) is illustrated in figure 2. This experimental closed loop mainly consists of three flow lines, i.e. gas stream (along the arrow  $\longrightarrow$ ), particle stream ( $\dashrightarrow$ ) and gaseous solid suspension stream ( $\dashrightarrow$ ). In the following explanation, the numbers in the circles correspond to those in figure 2. The gas is circulated by a diaphragm-type compressor (1). The gas flow rate is adjusted by a by-pass circuit valve and is measured by Venturi tube (6). The solid particles are supplied through a feed tank (20) to a screw feeder (8). The feed tank is connected between two ball valves (19) which are controlled for the prevention against the reverse flow of the suspension. The gaseous solid suspension emerging from the screw feeder cone enters vertically a heat transfer section (10), where the suspension flow is heated electrically and various data such as wall temperatures, fluid temperatures, heat fluxes and pressures are measured under a steady condition. Leaving the test section, the suspension flow is cooled near to a room temperature in

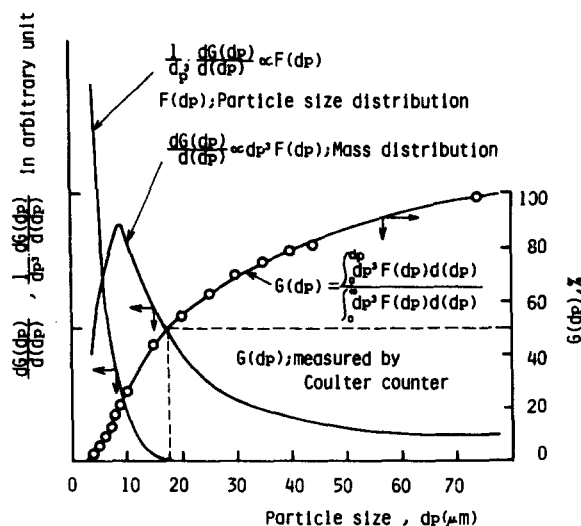


Figure 1. Particle size distribution.

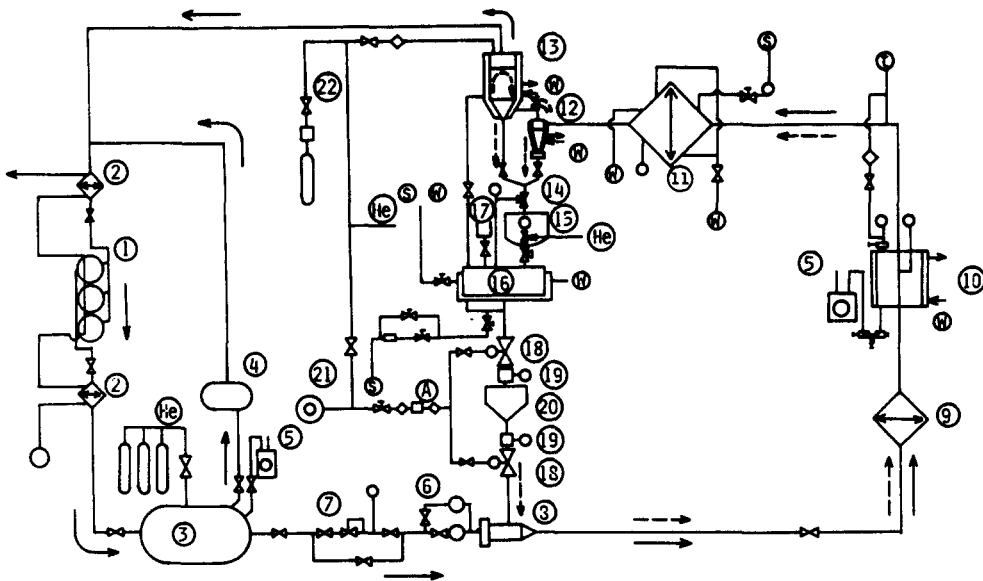


Figure 2. Flow diagram of gas solid suspension loop. (1) compressor; (2) after-cooler; (3) surge tank; (4) cushion tank; (5) vacuum pump; (6) flowmeter (Venturi tube); (7) flow regulator; (8) screw feeder; (9) preheater; (10) test section; (11) heat exchanger; (12) cyclone; (13) bag filter; (14) rotary valve; (15) particle measuring equipment; (16) ribbon blender; (17) powder supply; (18) ball valve; (19) particle level switch; (20) feed tank; (21) air compressor; (22) gas pulsar; (w) cooling water; (s) steam; (A) compressed air; (He) supply of He;  $\dashrightarrow$  particle stream;  $\longrightarrow$ , gas stream.

a heat exchanger which is made of coiled tubes submerged in a water bath (11). After flowing through the heat exchanger (11), the medium enters the cyclone separator (12), where the major amount of the particles is separated. The residual amount which has not been captured is collected by a bag filter (13) connected in series with the cyclone. Collected particles are sent to a weight measuring equipment of particles (15) through two rotary valves and accumulated in a conical hopper within it. The weight variation of the hopper containing the particles is recorded continuously and the solid flow rate is calculated from the slope of the recorded curve. When the weight of the hopper exceeds a certain value, a slide valve located at the bottom of hopper is opened and the particles fall into a ribbon blender (16).

#### Heat transfer test section

The details of the test section are illustrated in figure 3. Various considerations are taken in the heat transfer section to cope with a situation at high heat fluxes and high temperatures. The main heater is made of an Inconel pipe of 18 mm i.d. (denoted by  $D$ ), 0.75 mm in thickness and 1000 mm in length, which is equally divided into five segments (200 mm long regional pipe section) by water-cooled electrodes in order that the regional variation of the heating rate can be controlled. The pipe heater is wound by a fibrous insulator with an o.d. of about 90 mm and is also covered with asbestos tapes. This heater assembly is contained in an insulator vessel with a water jacket. Several tens of Pt-PtRh thermocouples are spot-welded at the middle point of each segment of the heating pipe and on the surfaces of electrodes. Moreover, seven pressure taps are welded on the test pipe to monitor the flow condition of the suspension medium.

A twisted tape, a sort of turbulence promoter, was inserted in the heating pipe in some later runs. The twisted tape is made of stainless steel plate of 2300 mm in total length (2000 mm long twisted part), 1 mm in thickness, 10 mm in width. The pitch is selected 200 mm and 400 mm (see figure 4). The tape end extends upstream 500 mm from the starting point of the heating section. Asbestos blocks ( $3 \times 10 \times 15 \text{ mm}^3$ ) are attached to the twisted part at intervals of 100 mm for preventing the tape from contacting the heater pipe.

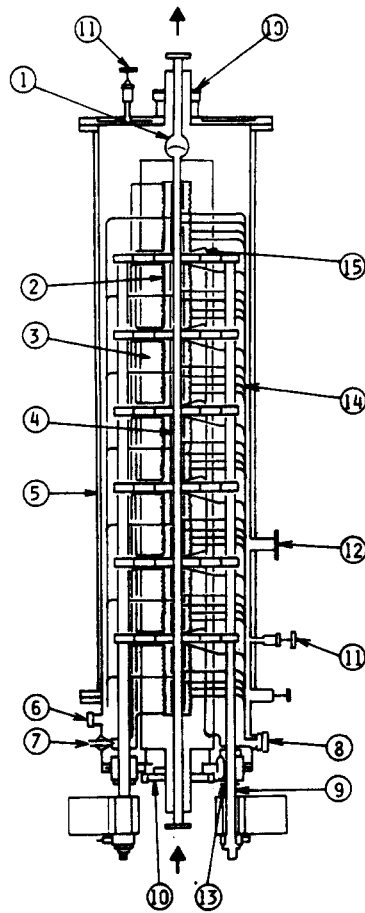


Figure 3. Detail of test section. (1) mixing chamber; (2) guard heater (removed); (3) asbestos insulator (removed); (4) pipe heater; (5) vessel with water jacket; (6) to pressure gauge; (7) electrode for guard heater (removed); (8) to thermo-recorder; (9) water cooled electrode; (10) teflon seal for test pipe; (11) leak valve; (12) to vacuum pump; (13) teflon seal for electrode; (14) thermocouple; (15) power lead.

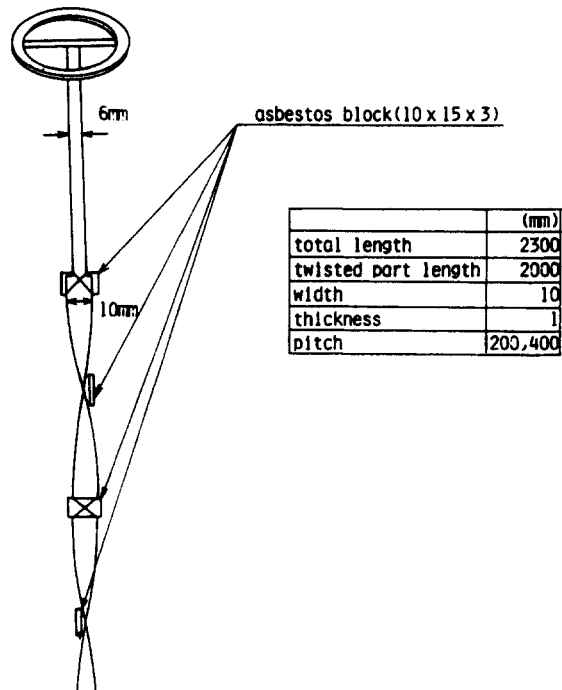


Figure 4. Detail of turbulence promoter (twisted tape).

### Experimental procedure

The experimental procedure for measuring heat transfer characteristics of the suspension medium is as follows:

- (1) Sufficient graphite particles are stored in the ribbon blender through a powder supply, and particles can be dried by steam flowing through the jacket of the blender, if so required.
- (2) The closed loop is exhausted of air by two vacuum pumps.
- (3) Helium gas is supplied into the loop up to a certain pressure.
- (4) The pump for water cooling system starts.
- (5) Helium is circulated by the diaphragm-type gas compressor and the mass flow rate of helium is regulated by the by-pass valve.
- (6) Particles are supplied from the ribbon blender to the feed tank.
- (7) The valve at the top of the tank is closed and the bottom valve is opened. The flow conditions of gaseous solid suspension are inspected at the glass tubes for visualization located in the loop. After it is confirmed that all the measurement items such as temperatures, gas and solid flow rates and pressures are held at steady state, the experimental data are recorded.

### 3. EXPERIMENTAL RESULTS AND DISCUSSION

#### Heat transfer without twisted tapes

Prior to the experiments of the forced convective heat transfer, heat losses were estimated through preliminary measurements by realizing a similar thermal condition in the insulator vessel. After the heat transfer test section is filled with tranquil helium to the same static pressure as that in the forced convective experiments and the same amount of cooling water is circulated in the test section as in the runs of heat transfer experiments, regional electrical inputs are measured under the condition that the temperature at the middle point of each segment of the heater pipe is adjusted to be constant. Figure 5 shows typical heat losses obtained for the static pressure at the test section of 0.197 MPa.

Next, some experiments of convective heat transfer are made with gas alone to check the

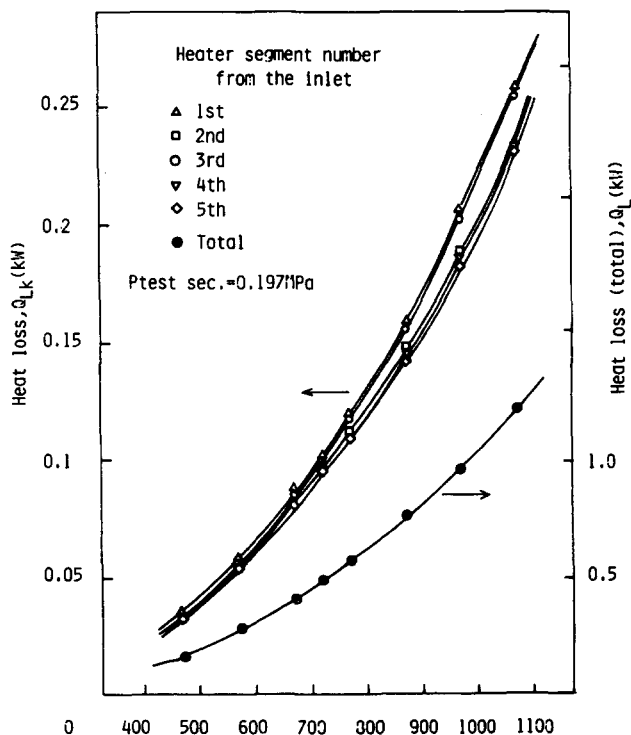


Figure 5. Typical heat loss of test section (400 mm pitch twisted tape).

characteristics of the heat transfer system. The heat loss in the case of the single phase flow reaches 27% of the total input at the most, when wall temperature,  $T_w$ , is 1173K and gas Reynolds number at inlet,  $Re_i$ , is  $1.0 \times 10^4$ . On the other hand, the maximum heat loss for the gaseous solid suspension experiments reduces to 14% of the total input, for example, at the particle loading ratio  $\Gamma$  of 4.06.

It is appropriate to evaluate local values of the heat transfer coefficient and Nusselt number, because the gaseous solid suspension enters the test section at room temperature and the ratio of wall to bulk temperatures of the suspension medium is much greater than unity. The local heat transfer coefficient,  $h_{bk}$  [ $W/(m^2 \cdot K)$ ], is calculated at the middle point of each regional heating segment of which the i.d.,  $D$ , is 18 mm and length,  $l$ , 0.2 m. The heat flux at  $k$ th segment from the inlet of the test pipe,  $q_k$  [ $W/m^2$ ], is

$$q_k = (Q_k - Q_{L,k})/A = Q_{N,k}/A \quad [1]$$

where  $Q_k$  is the electrical input,  $Q_{L,k}$  is the heat loss,  $Q_{N,k}$  is the net input and  $A = \pi \cdot l \cdot D$  is the heating area of the pipe heater segment. Meanwhile, a mixed mean temperature of the suspension at the  $k$ th segment,  $T_{bk}$ , is calculated by the following equation,

$$T_{bk} = \left( \sum_{j=1}^{k-1} Q_{N,j} + \frac{1}{2} Q_{N,k} \right) / (c_G G_G + c_S G_S) + T_i \quad [2]$$

where  $c$  is the specific heat for constant pressure, [ $J/(kg \cdot K)$ ] and  $G$  the mass flow rate, [ $kg/s$ ]. Here, the suffixes  $G$  and  $S$  mean the values which are related to gas and solid phases respectively and  $T_i$  is the inlet temperature of the gaseous solid suspension. The local heat transfer coefficient of the forced convection to the gaseous solid suspension,  $h_{bk}$ , is defined as

$$h_{bk} = q_k / (T_w - T_{bk}) \quad [3]$$

and the local Nusselt number,  $Nu_{bk}$ , is

$$Nu_{bk} = h_{bk} \cdot D / k_{bk} \quad [4]$$

where  $k_{bk}$  [ $W/(m \cdot K)$ ] is the thermal conductivity of the carrier gas based on the mixed mean temperature of the suspension. Entering gas Reynolds number,  $Re_i$ , is defined as

$$Re_i = u_i \cdot D / \nu_i = 4G_G / (\pi \cdot D \cdot \mu_i) \quad [5]$$

where  $u_i$  [ $m/s$ ] is the mean velocity,  $\mu_i$  [ $Pa \cdot s$ ] the coefficient of viscosity and  $\nu_i$  [ $m^2/s$ ] the kinematic viscosity of the gaseous phase at the inlet. The particle loading ratio,  $\Gamma$ , is the ratio of mass flow rate of solids,  $G_S$ , to that of gas,  $G_G$ , i.e.

$$\Gamma = G_S / G_G \quad [6]$$

The results of forced convective heat transfer to helium-graphite suspensions flowing vertically upward through the straight circular tube without a twisted tape are shown in figures 6–10 at the constant wall temperature. Experimental parameters in the current study are as follows,

$$\left\{ \begin{array}{l} \text{Wall temperature } T_w \text{ [K]; } 573, 723, 873, 973, 1073, 1173 \\ \text{Entering gas Reynolds number } Re_i \text{ [-]; } 1.0 \times 10^4, 1.5 \times 10^4, 2.0 \times 10^4 \\ \text{Particle loading ratio } \Gamma \text{ [-]; } 0-4. \end{array} \right.$$

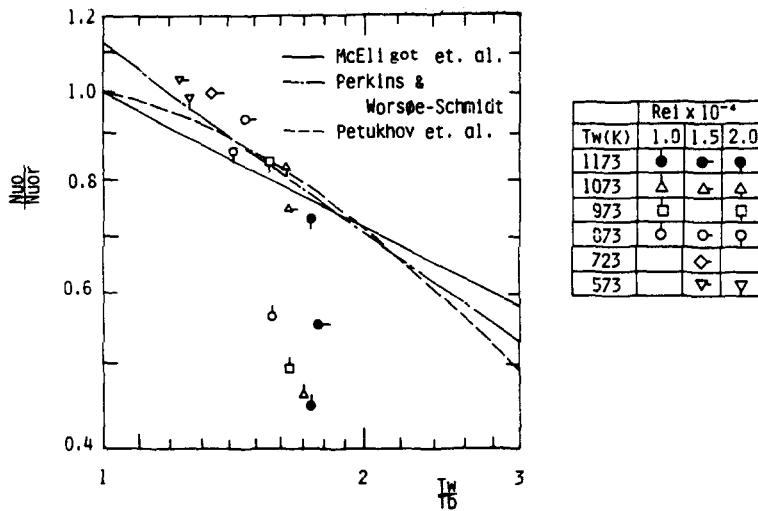
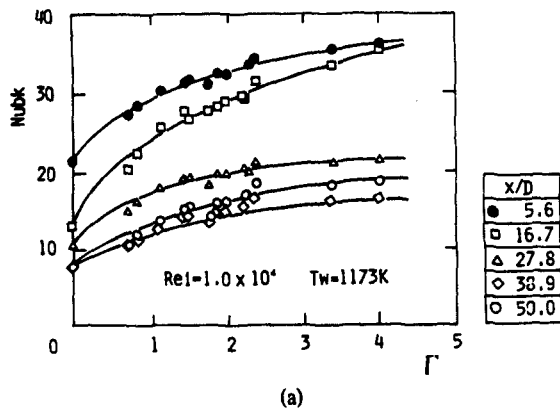
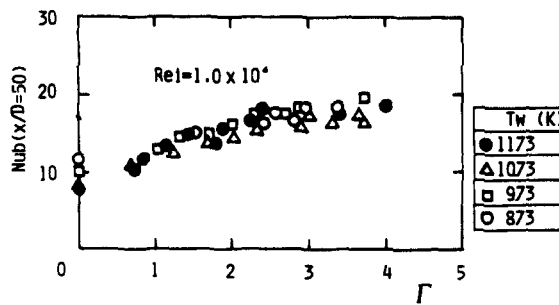


Figure 6. Experimental results of heat transfer for single phase flow.



(a)



(b)

Figure 7. Experimental results of gas solid suspension heat transfer at  $Re_i = 1.0 \times 10^4$ . (a) Variation in local Nusselt number with loading ratio ( $T_w = 1173K$ ). (b) Variation in Nusselt number at  $x/D = 50$  with loading ratio (Effect of  $T_w$ ).

In figure 6, the result of convective heat transfer to the single phase flow, i.e.  $\Gamma = 0$ , is compared with correlations proposed by McEligot *et al.* (1965), Perkins & Worsøe-Schmidt (1965) and Petukhov *et al.* (1966), where the variations of the physical properties are taken into account. The ratio of local Nusselt numbers,  $Nu_w/Nu_{0r}$ , at  $x/D = 50$  is plotted against the ratio of wall-to-bulk temperatures,  $T_w/T_b$ , in this figure, where the numerator,  $Nu_w$ , is the local Nusselt number obtained in this experiment and  $Nu_{0r}$  is the reference Nusselt number in the form of

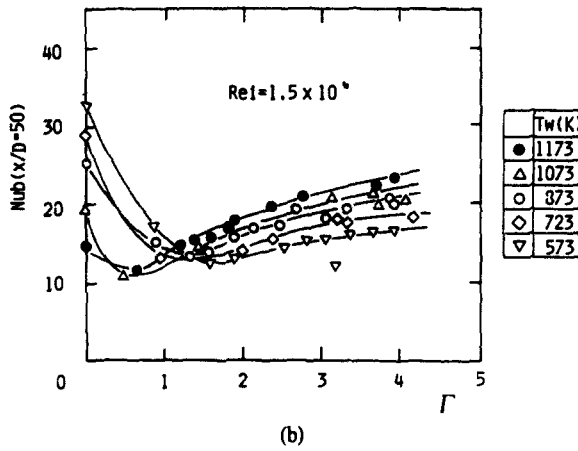
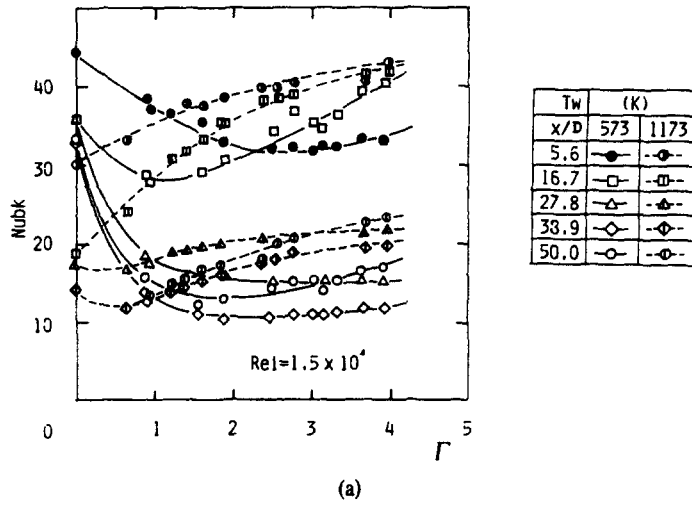


Figure 8. Results of gas solid suspension heat transfer at  $Re_i = 1.5 \times 10^4$ . (a) Variation in local Nusselt number with loading ratio ( $T_w = 573, 1173\text{K}$ ). (b) Variation in Nusselt number at  $x/D = 50$  with loading ratio (effect of  $T_w$ ).

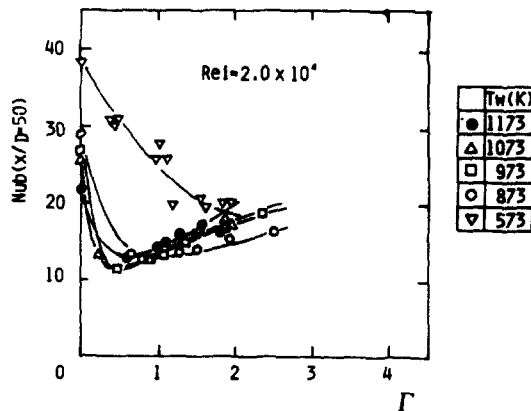


Figure 9. Results of gas solid suspension heat transfer at  $Re_i = 2.0 \times 10^4$ . Variation in Nusselt number at  $x/D = 50$  with loading ratio (effect of  $T_w$ ).



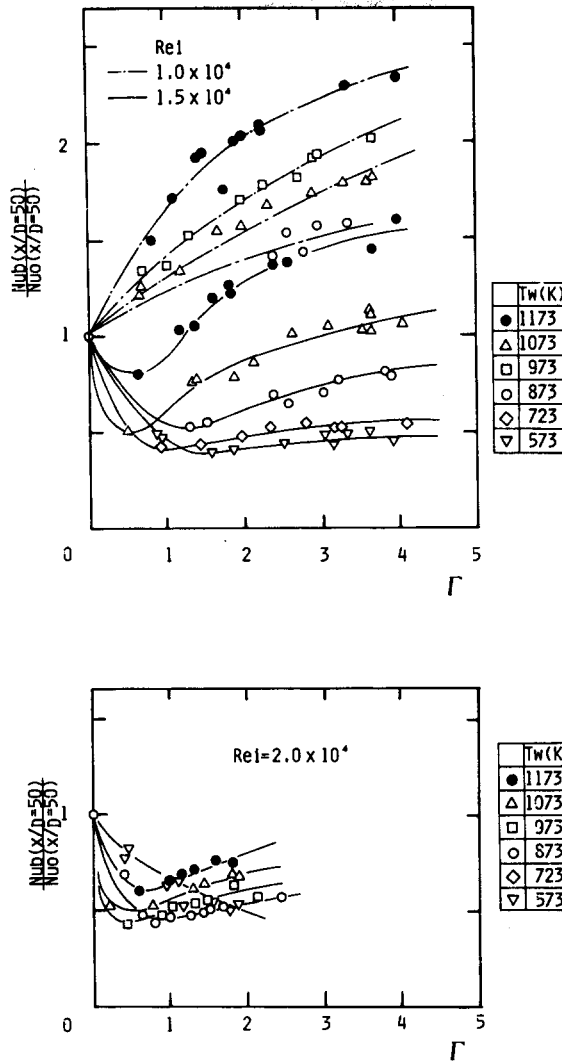


Figure 10. Variation of  $Nu_b/Nu_0$  at  $x/D = 50$  with loading ratio (effect of  $Re_i$  and  $T_w$ ).

$Nu_{0r} = 0.021 Re_b^{0.8} Pr_b^{0.4}$ , in which the values of  $Re_b$  and  $Pr_b$  are the same values of the experiment. According to the data in the case where the entering Reynolds number,  $Re_i$ , ranges from  $1.5 \times 10^4$  to  $2.0 \times 10^4$  except the run at  $T_w = 1173K$  and  $Re_i = 1.5 \times 10^4$ ,  $Nu_0$  almost agrees with the correlation proposed by Perkins *et al.* (1965). On the other hand, all the results obtained at  $Re_i = 1.0 \times 10^4$  including the run at  $Re_i = 1.5 \times 10^4$  and  $T_w = 1173K$  show that  $Nu_0$  is much lower than the correlations. This reduction can be attributed to the transition from the turbulent to the laminar region, because a characteristic value,  $K_\phi$ , in the current study is greater than the critical value of laminarization which Coon & Perkins (1970) proposed.

Figure 7 shows the result of heat transfer to the gaseous solid suspension at  $Re_i = 1.0 \times 10^4$ . In figure 7(a), which depicts the variation in the heat transfer along the axial direction of the test tube at  $T_w = 1173K$ , it is shown that the Nusselt number,  $Nu_{bk}$ , increases monotonically with the increase in the loading ratio  $\Gamma$ . This increasing tendency in  $Nu_{bk}$  is attributed to the turbulences induced by the fine particles and the augmented heat capacity of the suspension. Also, the unreasonable trend of  $Nu_{bk}$  between at  $x/D = 38.9$  and at  $x/D = 50.0$  is probably due to the heat loss at the end of the heating pipe. In figure 7(b), the effect of the wall temperature,  $T_w$ , on the heat transfer is shown, plotting the data of the local Nusselt number at the furthest location ( $x/D = 50$ ) in the wall temperature range from 873K to 1173K. This figure shows that

$Nu_{bk}$  increases only slightly with the rising in  $T_w$ , but it should be noted that the high heat flux reduces the forced convective heat transfer for the single phase flow. For example, McEligot *et al.* (1965) presented the correlation such as  $Nu_b = 0.021 Re_b^{0.8} Pr_b^{0.4} (T_w/T_b)^{-0.5}$ . Therefore, it might be considered that radiative heat transfer enhancement by the particulate phase owing to the rise in the wall temperature is compensated by the reduction effect of the ratio  $T_w/T_b$ .

The results of the gaseous solid suspension heat transfer at  $Re_i = 1.5 \times 10^4$  are shown in figure 8. In (a) of this figure, which is illustrated the same as figure 7(a) except for additional data in  $T_w = 573K$ , it shows that in the case of  $T_w = 573K$ ,  $Nu_{bk}$  at all of the five measuring points decrease to a certain value with increasing  $\Gamma$  and beyond this point  $Nu_{bk}$  has a trend to increase slowly. On the other hand, in the case of 1173K,  $Nu_{bk}$  in the entrance region such as  $x/D = 5.56$  and 16.7, which have a similar tendency as shown in figure 7(a), increases monotonically as the loading ratio,  $\Gamma$ , increases. At the downstream of the heater,  $Nu_{bk}$ , however, has a minimum value when  $\Gamma$  reaches about 0.5, and after exceeding this loading ratio the local Nusselt number becomes greater than the value for the single phase flow ( $\Gamma = 0$ ).

Figure 8(b) illustrates the effect of wall temperature on the local Nusselt number at  $x/D = 50$ . In this figure, it is shown that the heat transfer to the single phase flow reduces with increasing the wall temperature, while the local Nusselt number for the gaseous solid suspension in the range of the loading ratio above unity increases as the wall temperature rises. Therefore, the curves of  $Nu_b$  for varying wall temperatures intersect one another, and in the curve for  $T_w = 1173K$ ,  $Nu_b$  attains the same value as that of the single phase flow at  $\Gamma = 1$  and its increasing slope is the steepest among the curves.

Figure 9 shows the results of gaseous solid suspension heat transfer at  $Re_i = 2.0 \times 10^4$ , where  $Nu_b$  has a similar tendency as the results obtained at  $Re_i = 1.5 \times 10^4$ . That is, the loading ratio which gives us the minimum of the heat transfer becomes smaller and its rising gradient becomes steeper when the wall temperature increases.

It is well known that the data on the heat transfer of the flowing gaseous solid suspensions in circular tubes indicate two kinds of behavior against the loading ratio  $\Gamma$ . The current results of Nusselt number,  $Nu_b$ , for helium-graphite suspensions have the same tendency. It has been so far reported that the gaseous solid suspension Nusselt number increases monotonically with an increase of the loading ratio  $\Gamma$  in a small range of gas Reynolds number by some experimentalists, for example, Babcock & Wilcox Co. (1959), Nosov & Syromyatnikov (1966) and Wilkinson & Norman (1967). This augmentation effect on the heat transfer is attributed to fine particles which promote the turbulences of the fluid. On the other hand, the existence of the minimum value in  $Nu_b$  vs  $\Gamma$  has been experimentally confirmed by Farber & Morley (1957), Depew & Farber (1963) and Wahi (1977) in the case of higher gas Reynolds number, where the turbulent suppression by fine particles is presumably dominant over the turbulent promotion. Saffman (1962) examined the condition under which particles might stabilize the flow and Boothroyd (1967) experimentally showed that the eddy diffusivity to the momentum in the gaseous solid suspension appeared to have a minimum value in the range of small loading ratio, but the detail of the suppression mechanism is not clear.

In figure 10, the results on the heat transfer to the gaseous solid suspension flows shown in figures 7–9 are reproduced in the form of a conventional ratio of Nusselt numbers,  $Nu_b/Nu_0$ , where  $Nu_0$  is the Nusselt number of the single phase flow obtained experimentally at the same  $x$ ,  $T_w$  and  $Re_i$  and both Nusselt numbers are evaluated at  $x/D = 50$ . This figure shows that  $Nu_b$  at  $Re_i = 1.0 \times 10^4$  increases only slightly as the loading ratio or wall temperature increases. Moreover,  $Nu_0$  reduces to a great extent through the influence of high heat flux. Therefore, the dependence of the Nusselt ratio  $Nu_b/Nu_0$  on  $T_w$  and  $\Gamma$  is emphasized considerably. The contrary dependence of the Nusselt ratio on the wall temperature ( $T_w = 973$  and 1073K) seems to be due to the small increasing slope of  $Nu_b$  against  $T_w$ , which is also depicted in figure 7(b). On the other hand, the ratio,  $Nu_b/Nu_0$ , in the runs at  $Re_i = 1.5 \times 10^4$  and  $2.0 \times 10^4$  has a minimum value at a certain loading ratio and beyond the value increases monotonically as the loading

ratio,  $\Gamma$ , increases. It is clear that the rise in the wall temperature makes the loading ratio which minimizes the ratio,  $Nu_b/Nu_0$ , smaller and that the slope of the ratio of the Nusselt numbers becomes steeper with increase in the wall temperature.

#### Heat transfer with twisted tapes

As mentioned above, the current forced convective heat transfer to the gaseous solid suspension at high temperatures is reduced to a great extent especially in the range of small loading ratio,  $\Gamma$ . For the purpose of recovering this defect and making use of the large inertia forces of particles, for example, Boothroyd & Haque (1973) added fibrous balls into the suspension, Min & Chao (1966) controlled the motion of the particles with an electric field and Babcock & Wilcox Co. (1959) and Gorbis & Belyy (1970) inserted a turbulence promoter in a test tube.

Here, we discuss the results of the forced convective heat transfer to the gaseous solid suspension with two kinds of twisted tapes inserted in the test tube by turns.

A typical pressure drop of the suspension flow is illustrated in figure 11, when the test section is not heated. The friction factor,  $f$ , in this case is defined as,

$$\Delta p = 4f \frac{L}{D} \cdot \left( \frac{1}{2} \rho_G u_i^2 \right) \quad [7]$$

where  $L$  is the measuring length along the pipe ( $= 800$  mm),  $\Delta p$  is the pressure drop for  $L$  and  $\rho_G$  is the gas density. The friction factor,  $f$ , in the case where 400 mm pitch twisted tape is inserted in the test tube, increases by about six times as compared to that without the tape, when they are compared at  $\Gamma = 0$ . At the constant Reynolds number, the friction factors with tapes

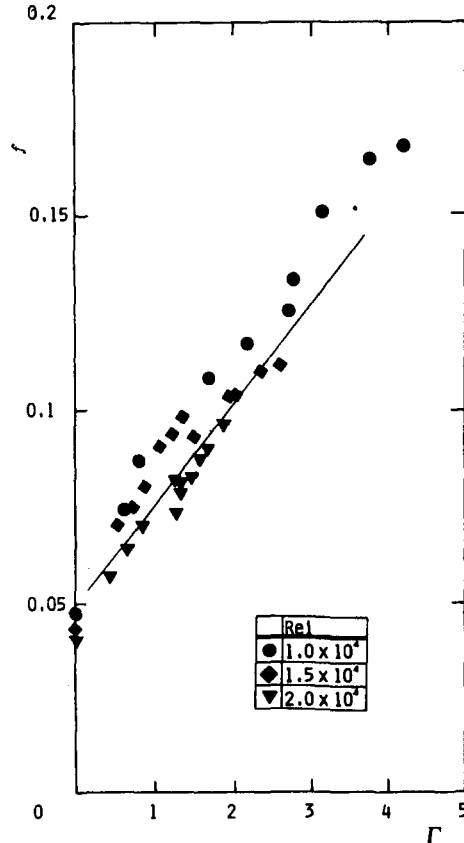


Figure 11. Variation in friction factor  $f$  with loading ratio (400 mm pitch twisted tape).

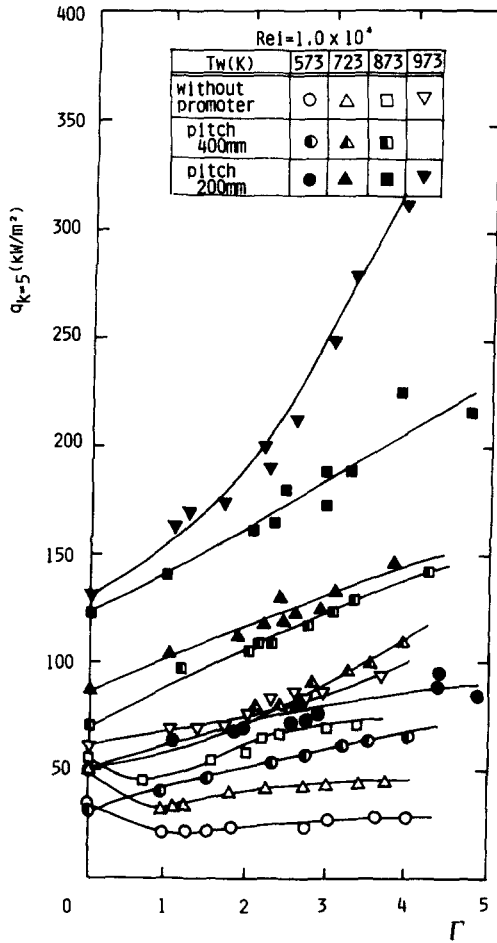


Figure 12.

Figure 12. Variation in local heat flux at  $x/D = 50$ ,  $q_k = 5$  with loading ratio ( $Re_i = 1.0 \times 10^4$ ).

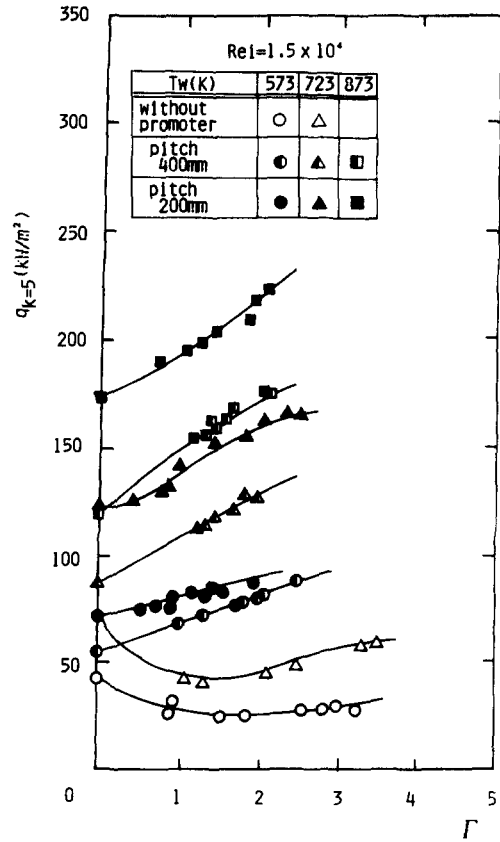


Figure 13.

Figure 13. Variation in local heat flux at  $x/D = 50$ ,  $q_k = 5$  with loading ratio ( $Re_i = 1.5 \times 10^4$ ).

increase linearly as  $\Gamma$  increases and its gradient is about 0.025. Also,  $f$  has a tendency to decrease with increase in  $Re_i$ .

The results of the heat transfer rate to the suspension flow with a twisted tape inserted in the tube are shown in figures 12–15, being compared with those without a tape. In the current experiment, it is found that heat transfer characteristics of the suspension using the twisted tapes are considerably better than the gaseous solid suspension alone. Moreover, at the point  $x/D = 50$ , which means the furthest measuring location along the test tube, the difference between the wall temperature and the mixed mean temperature of the gaseous solid suspension which is calculated from the heating input is rather small. Therefore, it is difficult to evaluate the local heat transfer coefficient or Nusselt number precisely. On the other hand, when the turbulence promoters were not used in the gas solid suspensions, the values of  $T_b/T_w$  at the exit of the test section attained to 0.7 at most. When a twisted tape is inserted in the flowing suspension, it might be considered that the particles collide with the heating surface more frequently owing to their centrifugal forces and change the structure of the turbulent boundary layer to a great extent. The augmentation of heat transfer to the gaseous solid suspension with a twisted tape is caused by the dynamics of the solids in the boundary layer, which seems to have a similar property to impinging and/or wall jets of gaseous solid suspensions as explained by Shimizu *et al.* (1979). In the current study, the wall temperature at each middle point of the

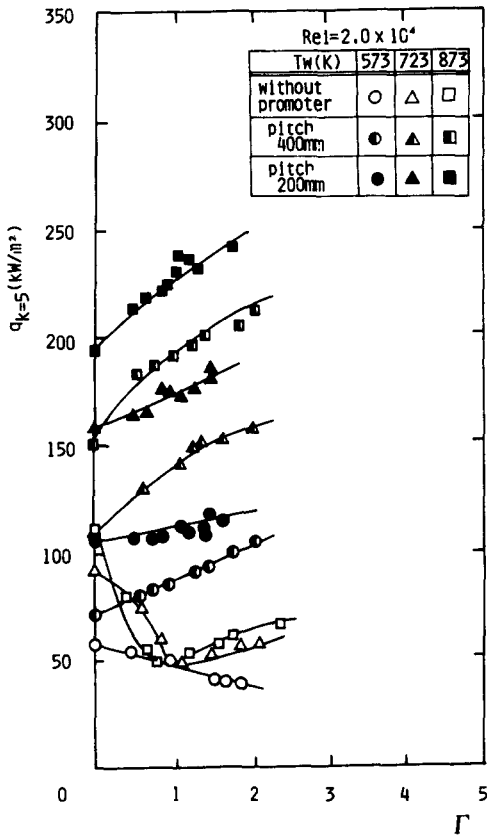


Figure 14.

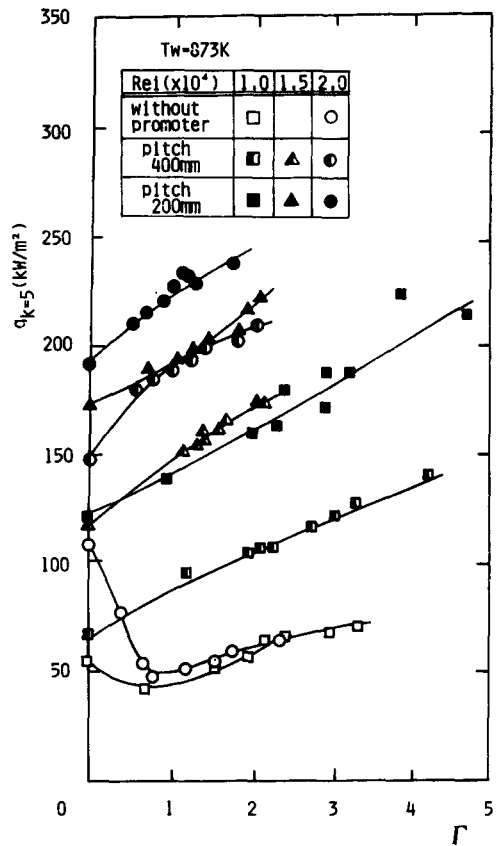


Figure 15.

Figure 14. Variation in local heat flux at  $x/D = 50$ ,  $q_k = 5$  with loading ratio ( $Re_i = 2.0 \times 10^4$ ).

Figure 15. Variation in local heat flux at  $x/D = 50$ ,  $q_k = 5$  with loading ratio ( $T_w = 873K$ ).

heater segments is monitored to make the wall temperature remain constant, so that in order to obtain the local heat transfer coefficient experimentally the distribution of the wall temperature along the tube should have been measured in more detail. In the following discussion, the main purpose is to check the augmentation effect of the twisted tapes on heat transfer characteristics and examine how much the experimental parameters such as wall temperature  $T_w$ , entering Reynolds number  $Re_i$  and loading ratio  $\Gamma$  influence the heat flux at the furthest segment of the heater pipe (fifth segment from the inlet),

$$q_{k=5} = (Q_{k=5} - Q_{L,k=5})/A = Q_{N,k=5}/A. \tag{8}$$

Figure 12 shows the variation in the local heat flux defined by [8] against the loading ratio at  $Re_i = 1.0 \times 10^4$ , where the wall temperature ranges from 573 to 973K and the loading ratio reaches about 5. The wall heat flux  $q_{k=5}$  with the twisted tapes increases monotonically with an increase in  $\Gamma$ , while the wall flux without them ranging in the wall temperature from 573 to 873K has a minimum at a certain value of loading ratio. Also, when we consider the effect of the tape pitch, the increase in wall heat flux with the 400 mm pitch tape is approximately parallel to that of 200 mm pitch tape, other things being equal. It is noted that the effect of wall temperature on the wall heat flux is considerable, for example, the wall heat flux at  $T_w = 973K$ ,  $\Gamma = 4$  and with 200 mm pitch tape is augmented to 3 times of that without the tape.

The variation in the local heat flux at  $x/D = 50$  at  $Re_i = 1.5 \times 10^4$  and  $2.0 \times 10^4$  with use of the twisted tapes are shown in figures 13 and 14, respectively, where the heat transfer rate of

gaseous solid suspensions with tapes is also predominantly higher than that without tapes and the same tendency depicted in figure 12 is confirmed.

Figure 15 summarizes the result of the wall heat flux when the wall temperature is fixed at 873K, showing the effects of the entering Reynolds number and loading ratio on the heat flux at  $x/D = 50$ . Of course, it is clear that the wall heat flux with use of the twisted tapes increases as  $Re_i$  increases and that the same tendency is observed at  $T_w = 573$  and 723K.

#### 4. CONCLUSION

The results of the experimental study of the forced convective heat transfer to flowing gaseous solid suspensions at high temperatures are presented. Results are reported for helium-graphite mixtures which are electrically heated with constant wall temperature conditions up to  $T_w = 1173$ K, flowing upward through a vertical circular tube; entering gas Reynolds number,  $Re_i$ , ranges from  $1.0 \times 10^4$  to  $2.0 \times 10^4$ , particle loading ratio,  $\Gamma$ , reaches about 4. The following conclusions are drawn from the current study.

(1) In the case of  $Re_i = 1.0 \times 10^4$ , the Nusselt number of the forced convective heat transfer to gaseous solid suspension,  $Nu_b$ , based on the local bulk properties increases monotonically with increase in the loading ratio. On the other hand, in runs of  $Re_i = 1.5 \times 10^4$  and  $2.0 \times 10^4$ , the Nusselt number of the suspensions has a minimum value at a low solid loading ratio.

(2) The ratio of the Nusselt number of the suspension to that of the gas alone increases considerably as the wall temperature increases in a range of high loading ratios.

The forced convective heat transfer to the suspension medium, especially in the range of small loading ratio,  $\Gamma$ , is reduced and it might be explained by the suppressive effect of fine particles on the fluid turbulence. To recover this defect and to make use of the large inertia forces of particles, two kinds of turbulence promoters (200 and 400 mm pitch twisted tapes) are inserted in flowing helium-graphite suspensions and the augmentation effect is successfully confirmed. The current results show that the local heat flux with the twisted tape increase significantly with an increase in the wall temperature  $T_w$  owing to the radiative effect to which the particulate phase might pertain.

#### REFERENCES

- BOBCK & WILCOCK Co. 1959 Final report on the gas suspension coolant project, AECBAW-1159.
- BOOTHROYD, R. G. 1967 Turbulence characteristics of the gaseous phase in duct flow of a suspension of fine particles. *Trans. Inst. Chem. Engrs* **45**, 297–310.
- BOOTHROYD, R. G. 1971 *Flowing Gas-Solid suspension*. Chapman & Hall, London.
- BOOTHROYD, R. G. & HAQUE, H. 1973 Improved convective heat transfer in a fluid with artificially modified turbulence. *J. Mech. Sci.* **1**, 61–72.
- COO, C. W. & PERKINS, H. C. 1970 Transition from the turbulent to the laminar region for internal convective flow with large property variations. *Trans. ASME J. Heat Transfer* **92**, 506–512.
- DEPEW, C. A. & FABER, L. 1963 Heat transfer to pneumatically conveyed glass particles of fixed size. *Trans. ASME J. Heat Transfer* **85**, 164–172.
- DEPEW, C. A. & KRAMER, T. J. 1973 Heat transfer to flowing gas solid mixtures. *Advan. Heat Transfer* **9**, 113–180.
- ECHIGO, R. & HASEGAWA, S. 1972 Radiative heat transfer by flowing multiphase medium, Part I. An analysis on heat transfer of laminar flow between parallel flat plates. *Int. J. Heat Mass Transfer* **15**, 2215–2534.
- ECHIGO, R., HASEGAWA, S. & TAMEHIRO, H. 1972 Radiative heat transfer by flowing multiphase medium, Part II. An analysis on heat transfer of laminar flow in an entrance region of circular tube. *Int. J. Heat Mass Transfer* **15**, 2595–2610.

- FARBER, L. & MORLEY, M. T. 1957 Heat transfer to flowing gas–solid mixture in a circular tube. *Ind. Engng Chem.* **49**, 1143–1150.
- GORBIS, Z. R. & BELYI, L. M. 1970 Aerodynamics and heat transfer of a counter-current gaseous suspension flowing onto decelerating spiral inserts. *Heat Transfer–Sov. Res.* **2**, 40–46.
- MC ELIGOT, D. M., MAGEE, P. M. & LEPPERT, G. 1965 Effect of large temperature gradients on convective heat transfer: the downstream region. *Trans. ASME J. Heat Transfer* **87**, 67–76.
- MIN, K. & CHAO, B. T. 1966 Particle transport and heat transfer in gas–solid suspension flow under the influence of an electric field. *Nucl. Sci. Engng* **26**, 534–546.
- MODEST, M. F., MEYER, B. R. & AZAD, F. H. 1980 Combined convection and radiation in tube flow of an absorbing, emitting and anisotropically scattering gas–particulate suspension. *Joint ASME/AIChE National Heat Transfer Conf.*, Paper No. 80-HT-27, ASME.
- NOSOV, V. S. & SYROMYATNIKOV, N. I. 1966 Laws of heat loss for finely dispersed flows. *Sov. Phys.–Dokl.* **10**, 672–674.
- PERKINS, H. C. & WORSØE-SCHMIDT, J. 1965 Turbulent heat and momentum transfer for at wall to bulk temperature ratio to seven. *Trans. ASME J. Heat Transfer* **87**, 1011–1031.
- PETUKHOV, B. S., KIRILLOV, V. V. & MAIDANIK, V. N. 1966 Heat transfer experimental research for turbulent gas flow in pipes at high temperature difference between wall and bulk fluid temperature. *Third Int. Heat Transfer Conf.*, Chicago, Paper No. 28, pp. 285–295.
- SAFFMAN, P. G. 1962 On the stability of laminar flow of a dusty gas. *J. Fluid Mech.* **13**, 120–128.
- SHIMIZU, A., ECHIGO, R. & HASEGAWA, S. 1979 Impinging jet heat transfer with gas–solid suspension medium. *Advances in Enhanced Heat Transfer*, 18th Nat. Transfer Conf., (Edited by CHENOWETH, J. M. et al.), ASME, pp. 155–160.
- SOO, S. L. 1967 *Fluid Dynamics of Multiphase System*. Blaisdell, New York.
- WAHI, M. K. 1977 Heat transfer to flowing gas–solid mixtures. *Trans. ASME J. Heat Transfer* **99**, 145–148.
- WILKINSON, G. T. & NORMAN, J. R. 1967 Heat transfer to a suspension of solid in a gas. *Trans. Inst. Chem. Engrs* **45**, 314–318.